Spin Structure Functions of Proton, Deuteron, and Neutron in the Resonance Region

A. Aghalaryan,[1] A. Ahmidouch,[2] R. Asaturyan,[1] F. Bloch,[3] W. Boeglin,[4] P. Bosted,[5] C. Carasco,[3] R. Carlini,[5] J. Cha,[6] J.P. Chen,[5] M.E. Christy,[7] L. Cole,[7] L. Coman,[4] D. Crabb,[8] S. Danagoulian,[2] D. Day,[8] J. Dunne,[6] M. Elaasar,[9] R. Ent,[5] H. Fenker,[5] E. Frlez,[8] D. Gaskell,[5] L. Gan,[10] J. Gomez,[5] B. Hu,[7] M. K. Jones,[5] J. Jourdan,[3] C. Keith,[5] C.E. Keppel,[7] M. Khandaker,[11] A. Klein,[12] L. Kramer,[4] Y. Liang,[7] J. Lichtenstadt,[13] R. Lindgren,[8] D. Mack,[5] P. McKee,[8] D. McNulty,[8] D. Meekins,[5] H. Mkrtchyan,[1] R. Nasseripour,[4] I. Niculescu,[5] K. Normand,[3] B. Norum,[8] D. Pocanic,[8] Y. Prok,[8] B. Raue,[4] J. Reinhold,[4] J. Roche,[5] D. Rohe,[3] O.A. Rondón,[8] N. Savvinov,[14] B. Sawatzky,[8] M. Seely,[5] I. Sick,[3] K. Slifer,[8] C. Smith,[8] G. Smith,[5] S. Stepanyan,[1] L. Tang,[7] S. Tajima,[8] G. Testa,[3] W. Vulcan,[5] K. Wang,[8] G. Warren,[3,5] F.R. Wesselmann,[8,11] S. Wood,[5] C. Yan,[5] L. Yuan,[7] J. Yun,[15] M. Zeier,[8] and H. Zhu[8]
(The Resonance Spin Structure Collaboration)

[1] *Yerevan Physics Institute, Yerevan, Armenia*
[2] *North Carolina A&T State University, Greensboro, North Carolina 27411*
[3] *Universität Basel, CH-4056 Basel, Switzerland*
[4] *Florida International University, Miami, Florida 33199*
[5] *Thomas Jefferson National Accelerator Facility, Newport News, Virginia 23606*
[6] *Mississippi State University, Mississippi State, Mississippi 39762*
[7] *Hampton University, Hampton, Virginia 23668*
[8] *University of Virginia, Charlottesville, Virginia 22903*
[9] *Southern University at New Orleans, New Orleans, Louisiana 70126*
[10] *University of North Carolina, Wilmington, North Carolina 28403*
[11] *Norfolk State University, Norfolk, Virginia 23504*
[12] *Old Dominion University, Norfolk, Virginia 23529*
[13] *Tel Aviv University, Tel Aviv, 69978 Israel*
[14] *University of Maryland, College Park, Maryland 20742*
[15] *Virginia Polytechnic Institute & State University, Blacksburg, Virginia 24061*

(Dated: June 26, 2012)

We measured the spin structure functions (SSFs) of proton and deuteron in the resonance region ($0.8 < W < 2.0$) at Q^2=1.3 GeV^2. The SSFs for the neutron were extracted by subtracting the *smeand* proton results from the deuteron data.

PACS numbers:

I. INTRODUCTION

introduction

II. EXPERIMENT

A. polarized electron beam

beam, raster, etc

B. DAQ

C. polarized targets

D. HMS

E. ENGINE

F. simulation program

(Is it here?)

III. RAW DATA ANALYSIS

The spin structure functions can be related to experimentally measured quantities through the use of asymmetries that are formed from the ratios of the differences to the sums of normalized yields for opposite beam helicities. The advantage of this approach for our experiment is twofold: factors that are independent of the beam helicity, such as the luminosity and detector acceptance, largely cancel out, and the measured asymmetries can be related to the spin asymmetries with minimal input of quantities not measured directly in the experiment.

The measured raw asymmetries for the parallel and perpendicular orientation of the target field relative to the beam $\varepsilon_{\parallel,\perp}(W)$ are related to the respective physics asymmetries $A_{\parallel,\perp}(W)$ by

$$\begin{aligned}\varepsilon_{\parallel,\perp}(W) &= \frac{N^+_{\parallel,\perp}(W) - N^-_{\parallel,\perp}(W)}{N^+_{\parallel,\perp}(W) + N^-_{\parallel,\perp}(W)} \\ &= f^{\parallel,\perp}(W) P_b^{\parallel,\perp} P_t^{\parallel,\perp} C_N(W) \\ &\quad (A_{\parallel,\perp}(W) - C_D(W)) \qquad (1)\end{aligned}$$

where $N^{+,-}_{\parallel,\perp}(W)$ represent the normalized yields,

$f^{\parallel,\perp}(W)$ represents the target dilution factor or fraction of events scattered off polarized hydrogen or deuterium nuclei, $P_b^{\parallel,\perp}$ and $P_t^{\parallel,\perp}$ are the the beam and target polarizations and $C_N(W)$ and $C_D(W)$ are corrections for the contributions of the polarized nucleons in nitrogen. All kinematics dependent quantities are integrated over the spectrometer's Q^2 acceptance for each W bin, because the spectrometer θ acceptance is too narrow to bin in Q^2.

Dropping the kinematic dependence and the field orientation indices in eq. (1), the measured physics asymmetry corrected for radiative processes can be written more compactly as

$$A^M = \frac{\varepsilon}{f P_b P_t C_N} + C_D \qquad (2)$$

In what follows we'll discuss in more detail the derivation of the right hand side of (1) and the calculation of the target dilution and nitrogen corrections.

A. Target dilution

The target dilution factor $f(W)$ represents the fraction of events scattered off polarized hydrogen or deuterium nuclei. Because f depends on W and the detector cannot distinguish among events coming from scattering processes on the different nuclear species present in the target, it is determined from a comparison between simulated rates and measured rates.

For the purpose of the simulation, the expected yields from all the target components for each beam helicity $N^+(W), N^-(W)$ for every bin in W can be written as

$$N^+(N^-) = \Phi(N_{15}\sigma_{15}^{+,-} + N_{1,2}\sigma_{1,2}^{+,-} + \sum N_A\sigma_A) \qquad (3)$$

where Φ is a flux factor, N_A are the numbers of scattering nuclei of mass A, $\sigma_A^{+,-}(W)$ represent polarized $e-A$ cross sections for nuclear species A (elastic or inelastic for H, quasielastic or inelastic for ^{2}H and N). All unpolarized nuclei in the target (He, Al, etc.) are lumped in the sum. The polarized cross sections terms of unpolarized cross sections σ_A and effective nucleon asymmetries $A_A^{p,n}(W)$ in nucleus A

$$\sigma_A^{+,-}(W) = \sigma_A(W)(1 \pm P_b P_A A_A^{p,n}(W)) \qquad (4)$$

where P_b is the beam polarization and P_A is the polarization of nucleus A.

For ^{15}N, which has only one polarizable proton, we can simplify this notation by using A_{15}^p. To avoid confusion with the spin asymmetries A_1 and A_2 we replace the indices 1 and 2 with p for hydrogen and d for deuterium. The yields for each helicity for the ordinary ammonia target then are

$$\begin{aligned} N^+(N^-) &= \Phi(N_{15}\sigma_{15}(1 \pm P_b P_{15} A_{15}^p) \\ &+ N_p\sigma_p(1 \pm P_b P_p A_p) + \sum N_A\sigma_A), \end{aligned} \qquad (5)$$

The ratio of the difference over the sum of yields for each helicity gives us the right hand side of our eq. (1)

$$\varepsilon = f_p P_b P_p C_N A_p \qquad (6)$$

with the customary definition of the proton dilution factor f_p

$$f_p = \frac{N_p\sigma_p}{N_p\sigma_p + N_{15}\sigma_{15} + \sum N_A\sigma_A} \qquad (7)$$

and the proton nitrogen correction

$$C_N = 1 + \frac{N_{15}\sigma_{15}A_{15}^p P_{15}}{N_p\sigma_p A_p P_p} \qquad (8)$$

The C_D correction term is absent for NH_3.

For ND_3 we need to include additional polarized contributions from unsubstituted ^{14}N and hydrogen which make up 2% and 1% of the nitrogen and deuterium nuclei, respectively. ^{14}N contributes with a polarized proton and a polarized neutron, and the helicity dependent yields are

$$\begin{aligned} N^+(N^-) &= \Phi\Big[N_{15}\sigma_{15}(1 \pm P_b P_{15} A_{15}^p) \\ &+ N_{14}\sigma_{14}\Big(1 \pm P_b P_{14}(A_{14}^p + A_{14}^n)\Big) \\ &\quad + N_p\sigma_p(1 \pm P_b P_p A_p) + N_d\sigma_d(1 \pm P_b P_d A_d) \\ &+ \sum N_A\sigma_A\Big]. \end{aligned} \qquad (9)$$

The corresponding ratio of the difference over the sum is

$$\varepsilon = f_d P_b P_d C_N (A_d - C_D) \qquad (10)$$

with the deuteron dilution factor

$$f_d = \frac{N_d\sigma_d}{N_d\sigma_d + N_{15}\sigma_{15} + N_{14}\sigma_{14} + \sum N_A\sigma_A} \qquad (11)$$

and the nitrogen and unsubstituted hydrogen corrections

$$C_N = 1 + \frac{N_{14}\sigma_{14}(A_{14}^p + A_{14}^n)P_{14}}{N_d\sigma_d A_d P_d} \qquad (12)$$

and

$$C_D = \frac{1}{C_N}\Big(\frac{A_{15}^p}{A_p}\frac{N_{15}\sigma_{15}}{N_d\sigma_d}\frac{P_{15}}{P_d} + \frac{N_p\sigma_p}{N_d\sigma_d}\frac{P_p}{P_d}\Big)A_p \qquad (13)$$

B. Packing Fraction

Before the determination of the dilution factors, we first need to determine a related factor for each target used in this experiment. Because the target cup was packed with solid ammonia beads (NH3 or ND3) and then filled with liquid helium, we determined the volume content of the ammonia in the target which we refer to the *packing fraction* (PF). Other materials near the target that contributed to the yield in the HMS are

FIG. 1: Radiative corrections to the measured asymmetries.

summarized in Table ??. The PFs are determined by comparing the data on carbon and ammonia targets with simulated results. Carbon data taken with the same kinematical conditions were compared with simulation to determine the normalization factor. Figure ?? shows the comparison between carbon data and simulation in order to determine the normalization. Next, we ran the simulation program on ammonia target with the same kinematical conditions as those for the production data with assumed PFs of 50% and 60%. Simulated yields obtained with PF=50 and 60% are compared with the data yields. The PF (in %) is extracted from the linear interpolation of those yields. To obtain the yields, the yield distribution was intergrated over the W region $1.2 < w < 1.5 (1.5 < w < 1.8)$ for $P_e = 4.8$ ($P_e = 4.0$) where the simulation agree with data well. Typical values of packing fractions for our targets are 50-60%. Figure ?? shows the comparison of data with simulation to extract the packing fraction. We take the weighted average of the two PFs obtained from the runs with two different momentum settings and take it as the PF of the target.

C. Determination of Dilution Factor

Once the PF is determined for each target, the simulation program is run once again with the PF that we found. After a large number of events are generated, the ratio proton yields (Z=1) and total yields (see Eq. 7) is calculated as a function of W, and that gives the dilution factor of a target. Figure?? shows the dilution factors of NH3 and ND3 targets.

[things need to be added: DF in elastic region, cuts used,]

D. simulation program

Should we put this section here or in experiment section?

E. Systematic Uncertainty

systematic uncertainties in PF and DF...

IV. PROTON RADIATIVE CORRECTIONS

An incident electron loses some fraction of its energy as it passes through the materials before and after scattering, as well as during the interaction itself. The procedure to account for these effects are known

Orientation	T_b	T_a
parallel	0.0246	0.0253
perpendicular	0.0256	0.0294

TABLE I: Material thickness in radiation lengths before and after the scattering for both target orientations.

as external and internal radiative corrections, respectively. The internal radiative corrections include corrections to the leading order Feynman diagram and can be spin-dependent. The external corrections are spin-independent (as long as the non-target material is unpolarized) and are dominated by the emission of brehmsstrahlung, with a small contribution arising from the Landau straggling of the electron.

The external radiative correction were applied following the formalism of Mo and Tsai [**?**], using the peaking approximation procedure of Ref. [**?**]. The internal radiative corrections utilized the Fortran based POLRAD [**?**] code which was updated to include a model of the RSS polarized data.

A. Elastic Tail Subtraction

The elastic peak has the lowest possible invariant mass and can radiate events to all higher mass states. It must therefore be subtracted before the inelastic radiative corrections are applied. The measured asymmetry contains a contribution from elastic tail as follows:

$$A_T^{\rm r} = \frac{\Delta_T^{\rm r}}{\Sigma_T^{\rm r}} \;=\; \frac{\Delta_{\rm in}^{\rm r} + \Delta_{\rm el}^{\rm r}}{\Sigma_{\rm in}^{\rm r} + \Sigma_{\rm el}^{\rm r}} \tag{14}$$

where the subscripts T,el and in refer to the total measured quantity, elastic and inelastic contributions respectively. The superscript r implies the the quantity is radiated. For example, $A_T^{\rm r}$ represents the measured asymmetry.

Because the asymmetries are not additive, we perform the tail subtraction on the polarized cross section $\Delta = \Sigma A$:

$$\Delta_{\rm in}^{\rm r} \;=\; \Delta_T^{\rm r} - \Delta_{\rm el}^{\rm r} \tag{15}$$

The measured asymmetry is related to the polarized cross section via:

$$A^{\rm r}_{\rm in} = \frac{\Delta^{\rm r}_{\rm in}}{\Sigma^{\rm r}_{\rm in}} \tag{16}$$

$$= \frac{\Delta^{\rm r}_{T} - \Delta^{\rm r}_{\rm el}}{\Sigma^{\rm r}_{\rm in}} \tag{17}$$

$$= \frac{\Sigma^{\rm r}_{T} A^{\rm r}_{T} - \Delta^{\rm r}_{\rm el}}{\Sigma^{\rm r}_{\rm in}} \tag{18}$$

$$= \left(\frac{\Sigma^{\rm r}_{T}}{\Sigma^{\rm r}_{\rm in}}\right) A^{\rm r}_{T} - \frac{\Delta^{\rm r}_{\rm el}}{\Sigma^{\rm r}_{\rm in}} \tag{19}$$

$$= \frac{1}{f} A^{\rm r}_{T} - Cel \tag{20}$$

where we have made the following definitions:

$$f = \frac{\Sigma^{\rm r}_{\rm in}}{\Sigma^{\rm r}_{T}} \tag{21}$$

$$C_{el} = \frac{\Delta^{\rm r}_{\rm el}}{\Sigma^{\rm r}_{\rm in}} \tag{22}$$

The radiative dilution factor f is completely determined by the model [?] of the unpolarized cross section Σ, and is the only part of the radiative correction to affect the statistical errors. C_{el} requires both the unpolarized model and knowledge of the elastic asymmetry [?] to form $\Delta^{\rm r}_{\rm el}$.

B. Inelastic Radiative Correction

The external material thickness was modeled as two radiators of thickness T_b and T_a placed before and after the target respectively. The relevent radiation lengths of RSS are listed in Table I.

After the elastic tail is subtracted, a fit was made to the RSS A_1 and A_2 data. A global model [?] of the unpolarized proton data was used to transform these fits directly into polarized cross sections as needed for the radiative corrections. The polarized cross section model was radiated and then compared to the measured data. An iterative procedure was used to adjust this model until the final radiated cross section agreed with the measured data. The difference between the Born and radiated asymmetry models was then applied directly to the measured inelastic data and is defined as C_{in}.

So the total radiative correction is given explictly by

$$A = \frac{A_{raw}}{f} + C \tag{23}$$

where C has both an elastic and inelastic contribution.

C. Systematic Uncertainties

The elastic form factors contributed 5% uncertainty to the tail subtraction, while the model-dependence of the inelastic radiative corrections was evaluated by performing the procedure with several different inelastic models, varying the A_1 and A_2 models independently. The additional models were the JLab Hall B fit [?] to world data excluding, and then including Eg1a [?] data, along with the AO [?], and the DMT [?] models.

D. Total Radiative Correction

The size of the radiative corrections and the related systematic uncertainy can be seen in Fig. 1.

V. PROTON ANALYSIS

(rss proton analysis)

VI. DEUTERON ANALYSIS

A. deuteron Radiative correction

B. Deuteron Results

deuteron apara, aperp, g1, g2, a1, a2

C. fit to data

D. systematics

E. duality

VII. EXTRACTING NEUTRON RESULTS

Spin structure functions (SSFs) of the neutron can be extracted from the proton and deuteron data from RSS. Because of the fermi motion of a nucleon inside deuteron, proton SSF needs to be smeared and then subtracted from deutron SSF. We follow the smearing procedures described in detail in [?], which is based on the work of Atwood-West [?]. Due to the Fermi motion, the invariant mass W and the energy transfer of the off-shell nucleon (W' and ν', respectively) differ from the on-shell ones, which can be calculated as a function of Fermi momentum. To obtain a smeared SSF of an on-shell one, the convolution of the on-shell quantity ($g_1^p(Q^2, W', \nu')$, etc) and the Fermi momentum distribution function is formed and integrated over the Fermi momentum space. We use the Paris wave function of the deuteron to get the deuteron Fermi momentum distribution. (We have two other WFs: Bonn and Hulthen-Yamaguchi, but any of the the WFs gives nearly the same smearing results because all three WFs are not so different from each other. Because $\Delta\sigma^p_{\parallel}$ and $\Delta\sigma^p_{\perp}$ are *linear* functions of g_1^p and g_2^p (see Eq.(4) of [?]), *smeared* cross section differences,

$\Delta\sigma_{\parallel}^{ps}$ and $\Delta\sigma_{\perp}^{ps}$, are first obtained using the Eq.(5) of the tech note [**?**], and then they are converted to give smeared proton SSFs, g_1^{ps} and g_2^{ps}. Figure 2 shows the

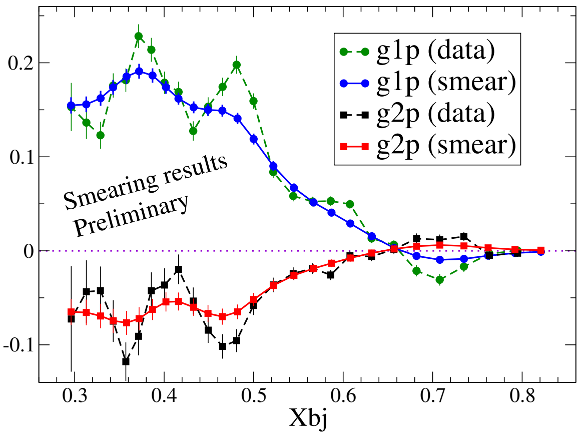

FIG. 2: Smearing effects on proton g_1 and g_2.

VIII. NEUTRON ANALYSIS

A. Neutron g_1 and g_2

We subtract the smeared g_1^{ps} from g_1^d to get g_1^n. Similarly for g_2^n extraction.

$$g_1^n = g_1^d/C_{depol} - g_1^{ps} \tag{24}$$

where $C_{depol} = 1 - 1.5\omega_D$ is the depolarization factor of the deuteron. $C_{depol} = 0.925$ with $\omega_D = 0.05$. The D-State correction factor is defined as $1/C_{depol}$. However,

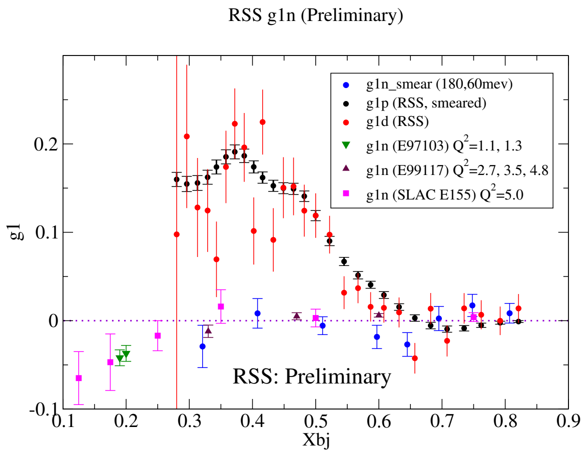

FIG. 3: Preliminary results of g_1^n extracted from RSS deuteron g_1 (data) and smeared proton g_1. Our results basically agree with the world data measured at the DIS regime, and are also consistent with zero.

the constant depolarization factor given above is valid

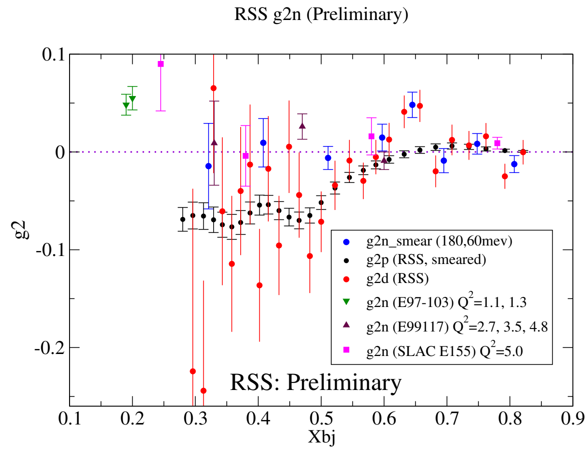

FIG. 4: Preliminary results of g_2^n extracted from RSS deuteron g_2 (data) and smeared proton g_2. Our results basically agree with the world data measured at the DIS regime, and are also consistent with zero except for one data point at $x_{BJ} = 0.65$.

for $x_{BJ} <\sim 0.7$ only. For higher x_{BJ} region, the depolarization factor deviates from 0.925 and start increasing as x_{BJ} becomes larger [**?**]. Figures 3 and 4 show the extracted smeared g_1^n and g_2^n. The bin width is 180 MeV ($x < 0.576$ or $W > 1.37$) and 60 MeV otherwise. Our preliminary results agree with world data measured in the DIS regime, and are basically consistent with zero except for one g_2^n data point at $x_{BJ} = 0.65$.

B. Neutron A_1 and A_2

Neutron A_1 and A_2 can be obtained from the extracted g_1^n and g_2^n.

$$A_1^n = (g_1^n - \gamma^2 g_2^n)/F_1^n \tag{25}$$
$$A_2^n = \gamma(g_1^n + g_2^n)/F_1^n, \tag{26}$$

where $\gamma = \sqrt{Q^2/\nu}$. Here, both g_1^n and g_2^n are smeared quantities. Therefore, we also need to have smeared F_1^n in order to extract A_1^n and A_2^n. Because the inelastic code by P. Bosted, F1F2IN06.f, outputs the unsmeared F_1^n, the code was modified slightly to return smeared F_1^n. Figure 5 shows the results of F_1 for proton, deuteron, and neutron. Smeared F_1 for proton and neutron are also plotted. The results of extracted A_1^n and A_2^n are shown in Figure 6. The bin size is 60 MeV. Comparison of different D-state corrections are also shown. The errors on A_1^n and A_2^n are calculated from the errors on g_1^n and g_2^n as well as 10% relative error on F_1^n that we *assumed.* However, I was told that the systematic error on F_1^n would be about 6% because the world data of deuteron used in the fit have statistical error of about 5%, and the proton data error is much smaller than that [**?**]. Our preliminary results are consistent with zero except for A_1^n at $W \sim 1.3 GeV$.

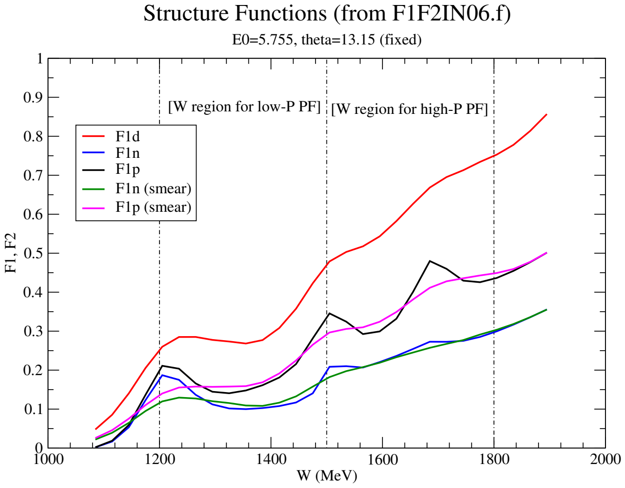

FIG. 5: Structure functions F_1 for proton, deuteron and neutron. These are outputs from F1F2IN06.f. Also plotted are smeared F_1^p and F_1^n from this code.

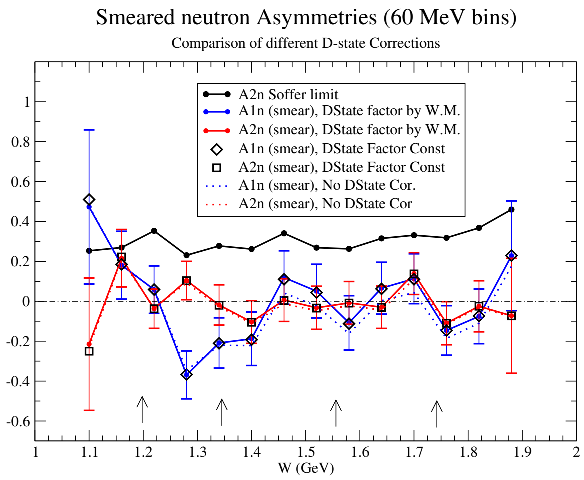

FIG. 6: Preliminary results of A_1^n and A_2^n (shown in blue and red solid lines, respectively). Also shown are the results using different D-State corrections (correction factor=1.0 (no correction), const factor=1/0.925, and full correction by Melnitchouk et al [?].) The arrows in the figure indicate the centroid positions of the resonances found from the fit to the RSS proton data [?].

IX. GLOBAL DUALITY OF THE NEUTRON

Is this needed?

X. CONCLUSION

conclusion

Also add appendix, showing table of proton, deuteron, neutron, data.

XI. ACKNOWLEDGEMENT

This work was supported by the U.S. Department of Energy,.... The Southeastern Universities Research Association operates the Thomas Jefferson National Accelerator Facility for the DOE under contract DE-AC05-84ER40150.

thank jlab staff, DOE, Wally Melnichouk for providing us his calculations.